PLASMA DYNAMICS

VI. PLASMAS AND CONTROLLED NUCLEAR FUSION*

A. Waves and Radiation

Academic and Research Staff

Prof. G. Bekefi	Prof. B. Coppi	Dr. D. J. Sigmar
Prof. W. P. Allis	Prof. E. V. George	Dr. A. Treves
Prof. A. Bers	Dr. R. Gajewski	J. J. McCarthy
Prof. S. C. Brown	Dr. P. A. Politzer	W. J. Mulligan

Graduate Students

R. J. Becker	L. Litzenberger	L. P. Mix, Jr.
H. Bhattacharya		M. L. Vianna

1. HIGH-SPEED NONLINEAR PLASMA WAVES†

When a wave propagates without changing its shape, particles move along constant energy orbits in the wave frame. Thus the distribution function is known at all points in phase space if it is specified at some position, say $x = x_o$. If we take the distribution function to be Maxwellian at $x = x_o$,

$$f(x_o, v) = n_o \sqrt{\beta/\pi}\, e^{-\beta v^2} = n_o \sqrt{\beta/\pi}\, e^{-\beta(u+w)^2}, \tag{1}$$

where $\beta = 2m/kT$, u is the phase velocity, and w is the particle velocity in the wave frame; the distribution function at other points is obtained as (1) evolves along constant energy orbits.

$$f(x, v) = n_o \sqrt{\beta/\pi}\, e^{-\beta(u+c)^2}, \tag{2}$$

where

$$c = w\sqrt{1 - 2e\phi/mw^2} \tag{3}$$

and ϕ is the wave potential.

This distribution function describes untrapped particles. Further specification of the trapped particle distribution must be made for a complete description. Several trapped particle distributions have been studied.[1,2] In the large phase velocity limit,

---

*This work was supported in part by the U.S. Atomic Energy Commission (Contract AT(30-1)-3980).

†This work was performed at the University of South Florida, Tampa.

plasma waves consistent with each of these distributions converge to the same asymptotic form (because in this limit the number of trapped particles becomes negligibly small and their exact distribution is thus inconsequential). This asymptotic limit is the subject of this report.

The electron density is given by

$$n = \int_{-\infty}^{\infty} dw\, f(x, w) = n_o \sqrt{\frac{\beta}{\pi}} \oint_{-\infty}^{\infty} dc\, \frac{|c|\, e^{-\beta(u+c)^2}}{\sqrt{c^2 + \eta}}, \tag{3}$$

where $\eta = 2e\phi/m$ and the broken integral means that the range $-\sqrt{-\eta} < c < \sqrt{-\eta}$ is excluded. This range represents excluded regions. The integrand is peaked near $c = -u$ with a width of order $\beta^{-1/2}$. For $\beta u^2 \gg 1$, the integrand is negligibly small near the excluded region and the range of integration may be extended from $-\infty$ to ∞ with little error. The asymptotic limit is insensitive to the details of the trapped distribution.

The density can now be expressed

$$n = n_o \sqrt{\frac{\beta\alpha}{\pi}} \int_{-\infty}^{\infty} dx\, \frac{|a-\chi|}{\sqrt{1 - 2a\chi + \chi^2}}\, e^{-\alpha\beta\chi^2}, \tag{4}$$

where

$$\alpha = u^2 + \eta, \qquad a = u/\sqrt{\alpha} = \left(1 + \frac{\eta}{u^2}\right)^{-1/2}, \qquad \chi = (u+c)/\sqrt{\alpha}.$$

Using the generating function for Gegenbauer polynomials[3]

$$(1-2\alpha t+\alpha^2)^{-v} \equiv \sum_{n=0}^{\infty} C_n^{(v)}(t)\, \alpha^n, \tag{5}$$

we can write

$$\frac{\chi - a}{\sqrt{1 - 2a\chi + \chi^2}} = \sum_{n=0}^{\infty} (n+1)\, C_{n+1}(a)\, \chi^n, \tag{6}$$

where $C_n(a) \equiv C_n^{(-1/2)}(a)$, $C_o = 1$, $C_1 = -a$ and the higher order Gegenbauer polynomials are related by the recursion relation

$$(n+2)C_{n+2} = (2n+1)aC_{n+1} + (1-n)C_n. \tag{7}$$

Term by term integration of (4) then gives

$$n = -n_o \sum_{m=0}^{\infty} \frac{(2m+1)\, C_{2m+1}(a)}{\alpha^m \beta^m} \frac{\Gamma(m+1/2)}{\Gamma(1/2)}. \tag{8}$$

A similar procedure yields the electron pseudopotential integral

$$\psi = \frac{n_o m e \alpha}{3\epsilon_o} \sum_{m=0}^{\infty} \frac{(2m+1)\, D_{2m+1}(a)}{\alpha^m \beta^m} \frac{\Gamma(m+1/2)}{\Gamma(1/2)}, \tag{9}$$

where

$$D_n(a) \equiv C_n^{(-3/2)}(a), \qquad D_o = 1, \qquad D = -3a$$

and

$$(n+2)D_{n+2} = (2n-1)a\, D_{n+1} + (3-n)D_n. \tag{10}$$

It is also possible to express (8) and (9) in terms of Legendre polynomials, although less compactly.

Retaining the first two terms of (8) gives

$$n = \frac{n_o}{\sqrt{1+\eta/u^2}} \left[1 - \frac{3}{4} \frac{\eta}{u^2} \frac{2kT}{mu^2} \frac{1}{(1+\eta/u^2)^2} \right]. \tag{11}$$

The first term in (11) is recognized as the result obtained by Akhiezer and Lyubarskii[4] for nonlinear waves in a zero-temperature plasma using the fluid equations. The second term, then, is a finite temperature correction. A zero-temperature plasma wave oscillates at the plasma frequency regardless of wavelength or amplitude. The correction term introduces a wavelength-dependent frequency shift (giving the Bohm-Gross[5] dispersion relation in the small amplitude limit) and an amplitude-dependent frequency shift (proportional to ϕ^2 for small amplitudes). To see this, we expand (11), in powers of η/u^2, retaining quadratic terms.

$$n = n_o \left[1 - \frac{\eta}{2u^2} \left(1 + \frac{3}{2\beta u^2} \right) + \frac{3}{8} \frac{\eta^2}{u^4} \left(1 + \frac{5}{\beta u^2} \right) \right]. \tag{12}$$

Poisson's equation is then

$$\nabla^2\phi + k_o^2\phi - \delta\phi^2 = 0, \tag{13}$$

where

$$u^2 k_o^2 = \omega_p^2 \frac{2\beta u^2 + 3}{2\beta u^2} \tag{14}$$

$$u^4 \delta = \omega_p^2 \frac{e}{m} \frac{3}{2} \left(\frac{\beta u^2 + 5}{\beta u^2} \right) \tag{15}$$

$$\omega_p^2 = \frac{n_o e^2}{m \epsilon_o}. \tag{16}$$

For small amplitudes, the term involving ϕ^2 is negligible and the wave frequency approaches $\omega_o = k_o u$ given by

$$\omega_o^2 = \omega_p^2 \left(1 + \frac{3}{2\beta u^2} \right), \tag{17}$$

which is the Bohm-Gross dispersion relation. For larger amplitudes, (13) has an exact solution in terms of elliptic functions. The frequency, correct to order ϕ^2, is given by

$$\omega^2 = \omega_o^2 \left(1 - \frac{15}{32} \frac{\eta_{max}^2}{u^4} \right). \tag{18}$$

For larger amplitudes, numerical solution of Poisson's equation using (8) shows that the waveform becomes increasingly nonsinusoidal, finally "breaking" at $\phi \sim \frac{mu^2}{2e}$, but at these large amplitudes trapped particles can no longer be neglected and the expansion given above is inapplicable, and a more complete analysis is required.[1]

R. W. Flynn, W. P. Allis

[Dr. R. W. Flynn is a member of the Department of Physics, University of South Florida, Tampa.]

References

1. W. P. Allis, in H. Feshbach and K. U. Ingard (Eds.), In Honor of Philip M. Morse (The M. I. T. Press, Cambridge, Mass., 1969).

2. H. K. Sen and P. M. Bakshi, Ninth International Conference on Phenomena in Ionized Gases, Bucharest (1969).

3. W. Magnos and F. Oberhettinger, Special Functions of Mathematical Physics (Chelsea, New York, 1949).

4. A. I. Akhiezer and G. Ya. Lyubarskii, Dokl. Akad. Nauk SSSR 80, 193 (1951).
5. D. Bohm and E. P. Gross, Phys. Rev. 75, 1851 (1949).

2. EVEN MOMENTS OF THE NONLINEAR DISTRIBUTION FUNCTION $f = n_o \sqrt{\beta/\pi}\, e^{-\beta(u+c)^2}$

The nonlinear distribution function $f = n_o \sqrt{\beta/\pi}\, e^{-\beta(u+c)^2}$ has proven to be useful in a variety of nonlinear wave problems.[1-3] Here $\beta = m/2kT$, u is the wave's phase velocity, $w = v - u$ is the velocity of an electron relative to the wave, and $\frac{1}{2} mc^2 = \frac{1}{2} mw^2 - eV$ is the total energy of an electron in the wave frame. V is the electrostatic potential and $\eta = eV/kT$.

This distribution function describes a Maxwellian distribution modified by the presence of an electrostatic potential, whose amplitude and waveform is determined by solving Poisson's equation self-consistently. We make the additional prescription that the distribution of trapped particles is the analytic continuation of the velocity-symmetric part of the untrapped distribution. We present here several expansions for velocity moments of this distribution. We will define I_p as the p^{th} velocity moment in the wave frame

$$I_p = \int_{-\infty}^{\infty} w^p f(w)\, dw. \tag{1}$$

When f is separated into its symmetric part, $f_s = \frac{1}{2} f(u+c) + \frac{1}{2} f(u-c)$, and its antisymmetric part, $f_a = \frac{1}{2} f(u+c) - \frac{1}{2} f(u-c)$, it is clear that only the symmetric part contributes to the even moments, and only the antisymmetric part contributes to the odd moments. Because the trapped particle distribution is the analytic continuation of f_s, even moments can be obtained without difficulty, even though f itself varies discontinuously in passing from the trapped to untrapped distributions. f_a, on the other hand, contains the discontinuity because it must equal zero for the trapped particles. Since the amplitude of the wave appears later in the calculation we do not know which particles are trapped and cannot, in general, find the odd moments before completely solving the problem. We can, however, find I_1, the wave-frame particle current, by using the continuity equation.

We will be primarily interested in $I_o = n$, the electron density, and $\frac{m}{2} I_2 = T$, the kinetic energy density in the wave frame. We can demonstrate that the pseudopotential integral

$$\psi = \int_0^{\phi} d\phi\, n = \int_0^{\phi} d\phi \int_{-\infty}^{\infty} dw\, f(w) \tag{2}$$

is equal to $2[T(\phi)-T(0)]$ by reversing the order of integration in (2).

In what follows, we will consider only even moments.

$$\frac{1}{n_o}\sqrt{\frac{\pi}{\beta}}\, f_s = \frac{1}{2}\, e^{-\beta(u+c)^2} + \frac{1}{2}\, e^{-\beta(u-c)^2} \tag{3}$$

$$= e^{-\beta c^2} \sum_{n=0}^{\infty} H_{2n}(\beta^{1/2}c)\, \frac{(\beta u^2)^n}{(2n)!}. \tag{4}$$

In obtaining Eq. 4 we have used the generating function for Hermite polynomials

$$e^{-z^2+2xz} = \sum_{n=0}^{\infty} H_n(x)\, \frac{z^n}{n!} \tag{5}$$

and the symmetry property $H_n(-x) = (-1)^n H_n(x)$. It is more convenient to express f_s in a way that explicitly displays its dependence on c^2 instead of c. To do this we express the Hermite polynomial in terms of a Laguerre polynomial, using the identity

$$H_{2n}(x) = (-1)^n\, 2^{2n} n!\, L_n^{-1/2}(x^2), \tag{6}$$

thus

$$\frac{\sqrt{\pi}}{n_o} f_s = e^{-\beta c^2} \sum_{n=0}^{\infty} \frac{(-1)^n\, 2^{2n} n!\, (\beta u^2)^n}{(2n)!}\, L_n^{-1/2}(\beta c^2). \tag{7}$$

The expression $2^{2n}n!/(2n)!$ can be expressed more compactly as $\dfrac{\Gamma\left(\frac{1}{2}\right)}{\Gamma\left(n+\frac{1}{2}\right)} = \dfrac{1}{\left(\frac{1}{2}\right)_n}$ using the identity

$$\Gamma(2z) = (2\pi)^{-1/2}\, 2^{2z-1/2}\Gamma(z)\, \Gamma\left(z+\tfrac{1}{2}\right)$$

and the Pochhammer notation

$$(z)_n = \frac{\Gamma(z+n)}{\Gamma(z)}.$$

Thus

$$\frac{1}{n_o}\sqrt{\frac{\pi}{\beta}}\,f_s = e^{-\beta c^2}\sum_{n=0}^{\infty}\frac{(-1)^n(\beta u^2)^n}{\left(\frac{1}{2}\right)_n}L_n^{-1/2}(\beta c^2).$$

We can now use the summation theorem below to separate $L_n(c^2)$ into explicit dependence on w^2 and η.

$$L_n^{a}(x+y) = e^{y}\sum_{k=0}^{\infty}\frac{(-1)^k}{k!}y^k L_n^{a+k}(x). \tag{8}$$

Using (8), we have

$$\frac{1}{n_o}\sqrt{\frac{\pi}{\beta}}\,f_s = e^{-\beta w^2}\sum_{n=0}^{\infty}\sum_{m=0}^{\infty}\frac{(-1)^n(\beta u^2)^n}{\left(\frac{1}{2}\right)_n}\frac{\eta^m}{m!}L_n^{m-1/2}(\beta w^2). \tag{9}$$

The p^{th} moment is obtained by multiplying (9) by w^p and integrating over w. This requires evaluation of

$$Q_p = \int_{-\infty}^{\infty} dw\, w^p\, e^{-\beta w^2}\, L_n^{m-1/2}(\beta w^2)$$

$$= \frac{1}{\beta^{(p+1)/2}}\,\frac{\Gamma\left(\frac{p+1}{2}\right)}{n!}\,(m-p/2)_n,$$

where we have used the standard integral

$$\int_0^{\infty} dx\, e^{-x}\, x^{\gamma-1}L_m^{\mu}(x) = \frac{\Gamma(\gamma)\,\Gamma(1+\mu+n-\gamma)}{n!\,\Gamma(1+\mu-\gamma)}$$

and the Pochhammer notation. Thus

$$I_p = \frac{n_o}{\beta^{p/2}}\,\frac{\Gamma\left(\frac{p+1}{2}\right)}{\Gamma\left(\frac{1}{2}\right)}\sum_n\sum_m\frac{\left(m-\frac{p}{2}\right)_n}{\left(\frac{1}{2}\right)_n}\frac{(-\beta u^2)^n\,\eta^m}{n!\,m!}. \tag{10}$$

Small Potential Expansion

Recalling the series defining the confluent hypergeometric function

$$M(a, b, z) = \sum_{n=0}^{\infty} \frac{(a)_n}{(b)_n} \frac{z^n}{n!}$$

we see that the p^{th} moment can be written

$$I_p = \frac{n_o}{\beta^{p/2}} \frac{\Gamma\left(\frac{p+1}{2}\right)}{\Gamma\left(\frac{1}{2}\right)} \sum_m M\left(m - \frac{p}{2}, \frac{1}{2}, -\beta u^2\right) \frac{\eta^m}{m!} . \tag{11}$$

It is often convenient to separate the m summation into a series with $m < p/2$ (for which this confluent hypergeometric function is proportional to a Laguerre polynomial) and a series for $m \geq p/2$. This gives

$$I_p = \frac{n_o}{\beta^{p/2}} \frac{\Gamma\left(\frac{p+1}{2}\right)}{\Gamma\left(\frac{1}{2}\right)} \sum_{a=1}^{p/2} \frac{a!}{\left(\frac{1}{2}\right)_a} L_a^{-1/2}(-\beta u^2) \frac{\eta^{(p/2)-a}}{\left(\frac{p}{2} - a\right)!}$$

$$+ \frac{n_o}{\beta^{p/2}} \frac{\Gamma\left(\frac{p+1}{2}\right)}{\Gamma\left(\frac{1}{2}\right)} \sum_{a=0}^{\infty} M\left(a, \frac{1}{2}, -\beta u^2\right) \frac{\eta^{a+p}}{(a+p)!} , \tag{12}$$

where we have used the identity

$$M(-n, \alpha+1, x) = \frac{n!\, L_n^{\alpha}(x)}{(2+1)_n} .$$

In particular, this gives

$$n = I_o = n_o \sum_{a=0}^{\infty} M\left(a, \tfrac{1}{2}, -\beta u^2\right) \frac{\eta^a}{a!} \tag{13}$$

for the electron density, and

$$I_2 = \frac{n_o}{2\beta} \left[1 + 2\beta u^2 + \sum_{a=0}^{\infty} M\left(a, \tfrac{1}{2}, -\beta u^2\right) \frac{\eta^{a+1}}{(a+1)!} \right] \tag{14}$$

for I_2, which is proportional to the wave-frame kinetic energy density, and the summation term is the pseudopotential.

Small Phase Velocity Expansion

Self-consistent plasma waves do not propagate at phase velocities less than approximately the thermal velocity. It is nevertheless useful to have a small u expansion of (10) for sheath formation studies, and so forth. If the m summation in (10) is performed first, we get

$$I_p = \frac{n_o}{\beta^{p/2}} \frac{\Gamma\left(\frac{p+1}{2}\right)}{\Gamma\left(\frac{1}{2}\right)} \sum_{n=0}^{\infty} \frac{(-\beta u^2)^n}{n!} B_n^p(\eta), \tag{15}$$

where

$$B_n^p(\eta) = \left(\frac{d}{d\eta}\right)^{n-1} \left[\left(\eta - \frac{p}{2}\right)^n e^{\eta}\right], \tag{16}$$

so $B_n^p(\eta)$ is a Boltzmann factor times an n^{th} polynomial in η.

R. W. Flynn, W. P. Allis

[This work was performed at the University of South Florida. Dr. R. W. Flynn is a member of the Department of Physics, University of South Florida, Tampa.]

References

1. W. P. Allis, Quarterly Progress Report No. 88, Research Laboratory of Electronics, M.I.T., January 15, 1968, pp. 121-129.
2. W. P. Allis, Quarterly Progress Report No. 92, Research Laboratory of Electronics, M.I.T., January 15, 1969, pp. 236-242.
3. W. P. Allis, in H. Feshbach and K. U. Ingard (Eds.), In Honor of Philip M. Morse (The M.I.T. Press, Cambridge, Mass., 1969), pp. 21-42.

3. THE MAXIMUM AMPLITUDE OF A NONLINEAR PLASMA WAVE

The Distribution Function

The distribution[1]

$$f = \frac{n_o}{\sqrt{\pi}} e^{-(u+c)^2} = \frac{n_o}{\sqrt{\pi}} e^{\eta - w^2} (\cosh 2uc - \sinh 2uc), \tag{1}$$

where

$$u = \sqrt{m/2kT}\, u'$$

$$w = v - u, \qquad \eta = eV/kT$$

and

$$c^2 = w^2 - \eta \tag{2}$$

are dimensionless variables representing phase velocity, electron velocity, potential, and electron energy, satisfies the collisionless Boltzmann equation identically. It gives a Maxwell-Boltzmann distribution for $u = 0$ and a linear Vlasov wave as $\eta \to 0$. It may therefore be used to extend the linear regime (except for Landau damping) to large amplitudes.

The distribution is plotted in Fig. VI-1, and exhibits surprisingly large discontinuities. The jump in f for $w = 0$, $c = \pm\sqrt{-\eta}$, offers no difficulties. As w goes through zero c is assumed to change sign also in order to maintain the proper limit as $\eta \to 0$.

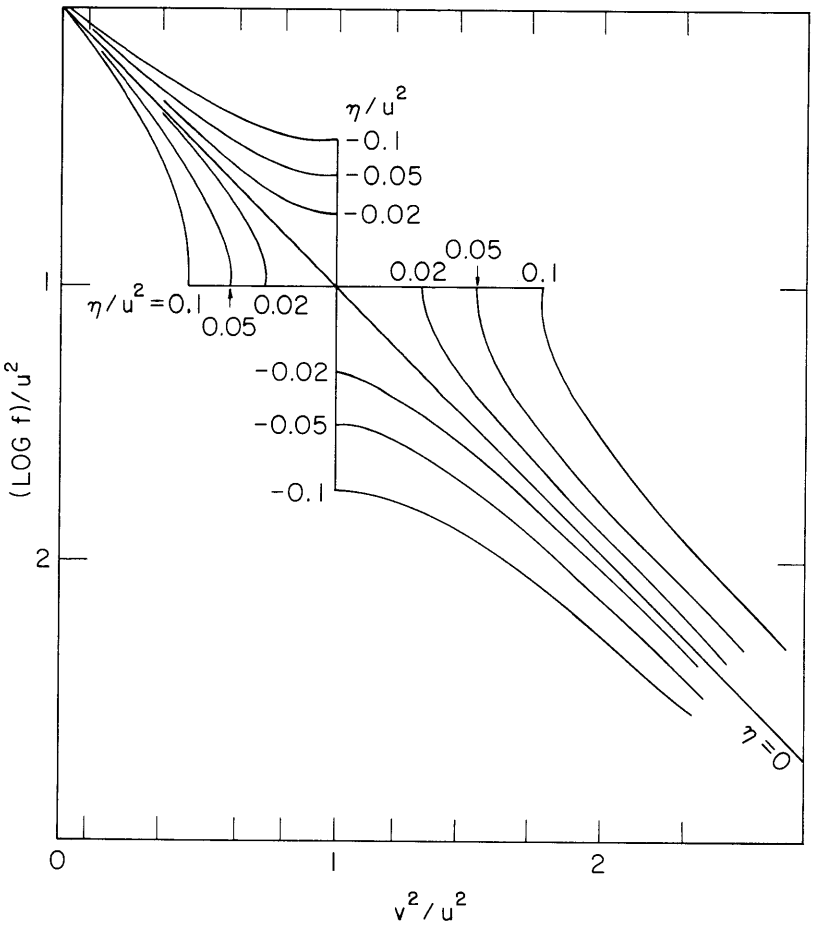

Fig. VI-1. Distribution $f = e^{(u+c)^2}$.

The gap between $w = \pm\sqrt{\eta}$ at $c = 0$ corresponds to electrons trapped below $\eta = 0$ in the potential well. The energy c^2 is negative in this region so that cosh 2uc - sinh 2uc becomes cos $2u|c| \pm i \sinh 2u|c|$. The imaginary term presents no difficulty because the reflection of electrons at the sides of the potential well of the wave symmetrizes the distribution and cancels this term. However, for large enough η the cosine term oscillates, and this seems unphysical. We shall make three alternative assumptions:
(a) For analytical purposes it is convenient to keep cos $2u|c|$. This is called "analytic continuation."
(b) We may set

$$\cos 2u|c| = 0 \quad \text{for} \quad c^2 < -(\pi/4u)^2 \tag{3}$$

and we shall call this the "empty well." Sen and Bakshi[2] use an empty well but set the limit at $c^2 = 0$. Our results differ from theirs only at small phase velocities.
(c) We may set

$$\cosh 2uc = 1 \quad \text{for} \quad c^2 < 0 \tag{4}$$

and shall call this the "filled well." The empty well is obviously not an equilibrium distribution. The filled well produces a Maxwell-Boltzmann distribution for positive potentials. One might wish to extend this distribution to the top of the well, but we have not done this.

The Electron Density

The distribution (1) has been integrated on the IBM 360/65 computer at the University of South Florida to obtain

$$n_-(u, \eta) = \int_{-\infty}^{+\infty} f \, dw \tag{5}$$

and the results are shown on Fig. VI-2.

For $u = 0$, $n_- = n_o e^{\eta}$. For slow waves $u < 0.926$ the density n_- has a maximum at positive potentials, as might be expected for trapped particles, but for $u > 0.926$ the maximum occurs at negative potentials. It is characteristic of free-streaming electrons that their velocity is less and therefore their density greater at more negative potentials. Eventually, the smaller number of electrons reaching a negative potential outweighs the greater density of those that do reach it and the density drops back through n_o at approximately $\eta_{1m} = -1.25\, u^2$.

On the positive potential side, one example ($u = 2.5$) of the analytic assumption is given to show the nature of the oscillations due to cos $2u|c|$. They become large for $\eta > u^2 - 1$. The empty wells are shown in Fig. VI-2b and the filled wells in Fig. VI-2c.

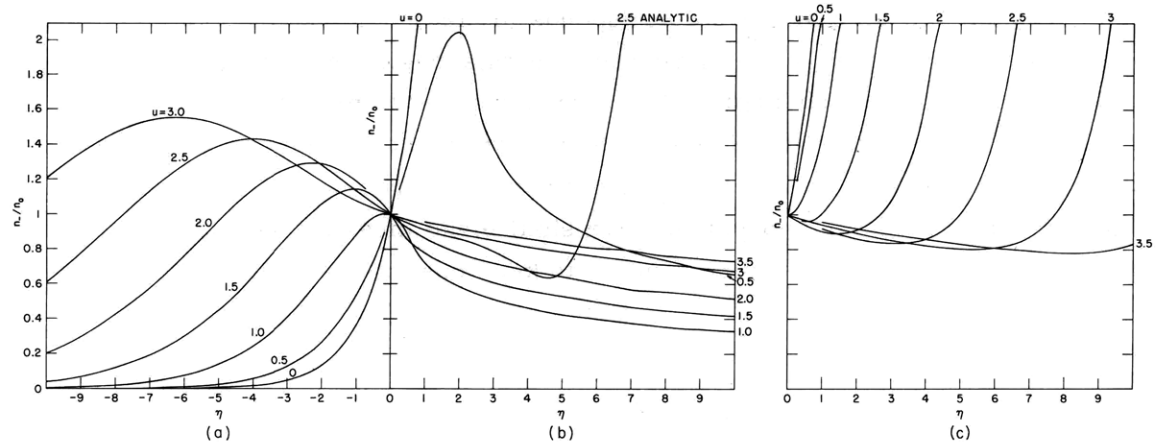

Fig. VI-2. Electron density n_-, (a) at negative potentials, (b) with empty well, (c) with filled well.

The former decrease roughly as $1/\sqrt{\eta}$, the latter decrease first then increase due to the Boltzmann factor e^{η} and cross $n_- = n_o$ around $\eta_{2m} = u^2 - 1$. It is seen that the analytic continuation is quite satisfactory for small amplitude waves, but must be discarded for amplitudes close to the maximum for filled wells.

The Pseudopotential

The pseudopotential is defined by

$$\psi(\eta) = \int_0^{\eta} \frac{n_+ - n_-}{n_o}\, d\eta = \frac{E_o^2 - E^2}{4\omega_o^2}, \tag{6}$$

the second equality following from Poisson's equation. Thus $E(\eta)$ implicit in this equation satisfies exactly the Vlasov equations. The integral has been evaluated by the computer with the assumption $n_+ = n_o$ and the results are shown in Fig. VI-3. The effect of this assumption is discussed elsewhere. Montgomery and Joyce[3] have shown how to interpret these plots by analogy with force potentials. If the pseudopotential forms a well and a horizontal line cuts it at η_1 and η_2, an oscillation is possible between these voltages. The field $E = 0$ at both intersections so that average space charge neutrality is assured, and E^2 is given at any point by the height of the line above the curve. If the curvature is such that $\psi(\eta)$ forms a hill instead of a well, no periodic wave is possible.

For $u > 0.926$ all these plots show positive curvature at $\eta = 0$ and hence waves are possible. However, the pseudopotential curves have a maximum at $\eta_{1m} \approx -1.25\, u^2$ and therefore no wave exists whose negative potential is beyond this limit. This is the point at which $n_- = n_o$ and consequently $n_- = n_+$ and $\rho = 0$. Beyond this

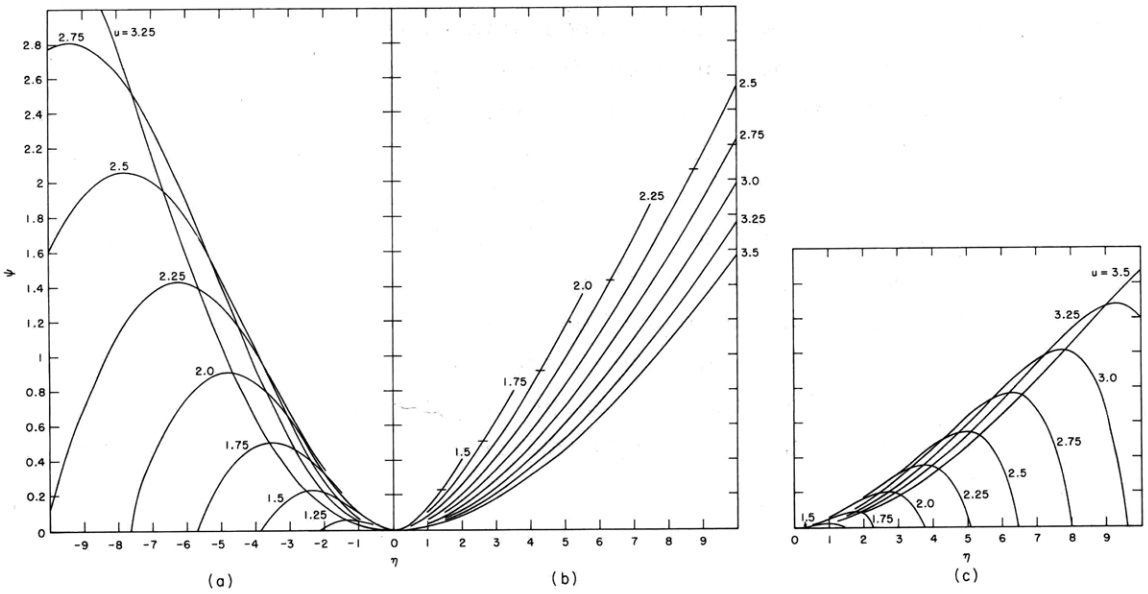

Fig. VI-3. Pseudopotential (a) at negative voltages, (b) for empty well, (c) for filled well.

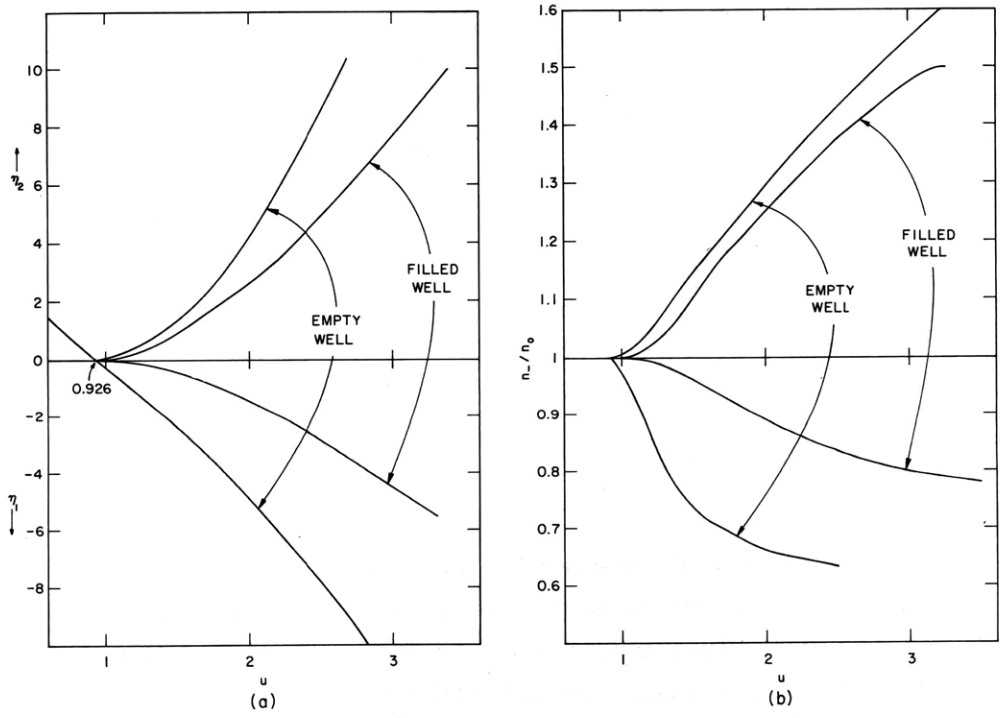

Fig. VI-4. (a) Maximum voltage amplitude.
(b) Maximum density amplitudes.

potential too many electrons would be trapped so that space charge would be positive where the potential has a minimum, which is not self-consistent. For an empty well the pseudopotential rises continuously for positive potentials so there is always an η_2. Both η_{1m} and η_2 are plotted in Fig. VI-4 to show how the maximum amplitude of a wave increases with the phase velocity. For a filled well the pseudopotential has a maximum on the positive side too, and this maximum is lower than that at the negative potential. It is the positive potential which limits a filled well, and indeed it does so because the Boltzmann factor puts more electrons in the well than there are ions available to give the required positive space charge. For a slightly less filled well the maxima on both sides can have the same height, and in that case a shock solution is possible. Trapping increases the wavelength (the curvature of ψ is less for the filled well) and eventually kills the wave.

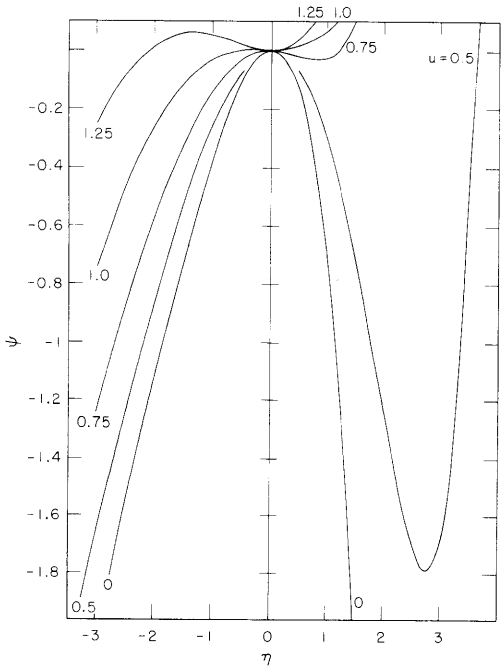

Fig. VI-5. Pseudopotential for small phase velocities.

Figure VI-5 shows the pseudopotential for slow waves $u < 0.926$. There are clearly no waves around $\eta = 0$ as the curvature is wrong, but the curves do have a minimum at a small positive potential. This indicates the existence of wave solutions satisfying the Vlasov equations but with both maximum and minimum potentials positive. It is possible that these represent moving striations, but it will be necessary to include ion motion before this is understood.

W. P. Allis, R. W. Flynn

[This work was performed at the University of South Florida. Dr. R. W. Flynn is a member of the Department of Physics, University of South Florida, Tampa.]

References

1. (a) W. P. Allis, Quarterly Progress Reports No. 88, Research Laboratory of Electronics, M. I. T., January 15, 1968, pp. 121-129; No. 92, January 15, 1969, pp. 236-242.
   (b) W. P. Allis, in H. Feshbach and K. U. Ingard (Eds.), In Honor of Philip M. Morse (The M. I. T. Press, Cambridge, Mass., 1969), pp. 21-42.
   (c) H. K. Sen and P. N. Bakshi, Ninth International Conference on Phenomena in Ionized Gases, Bucharest, 1969.

2. Loc. cit.

3. D. Montgomery and G. Joyce, J. Plasma Physics 3, 7 (1969).

VI. PLASMAS AND CONTROLLED NUCLEAR FUSION*

C. Plasma Diagnostics

Academic and Research Staff

Prof. G. Bekefi
Prof. E. V. George
Dr. P. A. Politzer

1. STARK PROFILES OF THE He I 4471 Å LINE AND OF ITS TWO FORBIDDEN COMPONENTS, MEASURED IN A LASER-PRODUCED PLASMA

Introduction

Stark profiles of allowed spectral lines emanating from dense plasmas and interacting with neighboring forbidden transitions have recently been calculated for a few special cases.[1-3] Subsequently, experiments were undertaken to verify the underlying theoretical assumptions and to open the way for new diagnostic methods. At relatively low plasma densities, where the widths of the allowed and forbidden components are small compared with their wavelength separation, conventional theory was shown to be inadequate around the forbidden component.[4] This failure was ascribed[5] to the fact that theory neglects the dynamics of the perturbing ions. Indeed, when proper allowance was made for ion motions, great improvements between the corrected theory and experiment were reported.[6,7] At higher densities, where the allowed and nearby forbidden lines overlap strongly, the effect of ion motions on the line profile should be entirely negligible, and any failure of the theory to reproduce the experimental profiles would have to be ascribed to some other cause. Recent measurements of helium line profiles made in this regime of densities show somewhat conflicting results. In one of these works,[8] made at a plasma density of $\sim 1 \times 10^{16}$ cm^{-3}, experiment and theory are said to be in fair agreement. In the other work,[9] however, significant departures are observed at densities 3×10^{16} to 1×10^{17} cm^{-3}: the separation between the peaks of the allowed and forbidden lines is not as large, and the dip between them not as deep, as theory would have it.

As a result of these conflicting observations, we have undertaken an independent experiment to see whether at high plasma density a genuine discrepancy indeed exists between experiment and theory. In our experiment we generate the plasma by means of a repetitive CO_2 laser which produces some 10 to 15 plasma pps. This allows us to scan the optical line profile continuously with good time and space resolution and thus

*This work was supported by the U.S. Atomic Energy Commission (Contract AT(30-1)-3980).

to free the experiment from the usual problems of shot-to-shot variations. We study the profiles of the strongly overlapping allowed line 2^3P-4^3D at 4471 Å and the near forbidden component 2^3P-4^3F at 4470 Å, for densities of 3.4×10^{16} cm^{-3} and 5.0×10^{16} cm^{-3}. We observe disagreements with theory similar to those reported by Nelson and Barnard.[9] On the other hand, the profile of the distant forbidden 2^3P-4^3P transition at 4517 Å, which interacts but weakly with the aforementioned two lines, agrees very well with theory. Although this line has received little attention from the experimentalists, it appears to have potential assets in the diagnostics of dense plasmas.

Experimental Results

Detailed descriptions of the experimental setup, reduction of data, and properties of the optically generated plasma are given elsewhere.[7, 10] The plasma is produced by a transversely excited atmospheric pressure (TEA) CO_2 laser. This laser yields 1-2 MW pulses of radiation at a wavelength of 10.6 μ. The pulse duration is approximately 200 ns and the repetition rate ~12 pps. The laser radiation is focused into a gas cell by means of a 3.8 cm focal length germanium lens. The cell is filled with spectroscopically pure helium to a pressure of 3/4 atm. The light from the helium plasma generated by the laser pulses is focused by means of a condensing lens onto the slits of a 0.5 m spectrometer provided with a motor-driven wavelength scan (Jarrell-Ash, Model 83-020) and a photomultiplier output. The output signal from the photomultiplier is fed into a boxcar integrator (PAR Model 160) and then to graphic display equipment. The boxcar gate width is typically 250 ns and thus represents the time resolution of our measurements. The gate can be set to any desired time delay relative to the time the laser is fired. This enables us to probe the entire afterglow history of the slowly decaying plasma. All measurements reported in this paper are made at a fixed time of 5 μs.

At this time the plasma is in the form of a cigar, about 0.6 cm long and 0.2 cm in radius. Although the light appears to be emitted quite symmetrically about the major axis of the cigar, the emission is very inhomogeneous, suggesting the existence of strong radial density and temperature gradients. For that reason, the line shape and intensity of all spectral lines in question are measured at 20 different lateral positions with a spatial resolution of 0.01 cm and the results Abel-inverted by means of a computer-generated program. This yields "true" line profiles at any desired radial distance from the plasma axis.

To obtain the radial distribution of the plasma density we make use of the isolated 2^3P-4^3S line of neutral helium centered at 4713 Å. This is done by computer-fitting the theoretical Stark broadened line profile to the experimental profiles (which were first Abel-inverted as described above). As an independent check, we also determine

the density from an analysis of the 2^1P-3^1D line at 6678 Å. The two sets of measurements agree to better than 15% at all radial plasma positions studied. The electron temperature and its radial distribution are deduced from the intensity ratio of the He II 4686 Å line and the He I 5876 Å line.

Since self-absorption of radiation could invalidate many of the above (and succeeding) interpretations, a careful study is made of this effect. Light emitted by the plasma in a direction away from the spectrometer slits is reflected back into the plasma by means of a spherical mirror. Measurement of the relative increase in the spectrometer output gives the absorptivity of the medium at any desired wavelength. In this way we find that at the time of observation (5 μs in the afterglow) self-absorption of all lines employed is negligible, with the exception of the strong 5876 Å line of He I. The mild

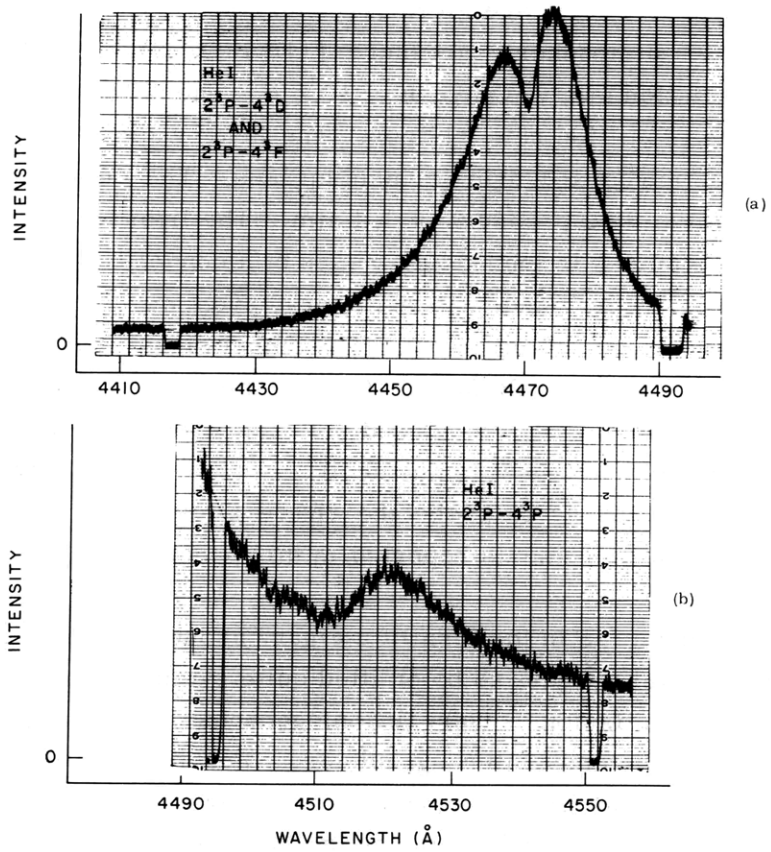

Fig. VI-6. The measured intensity profiles of the allowed 2^3P-4^3D He I line and the forbidden 2^3P-4^3F line (a), and the forbidden 2^3P-4^3P line (b). The measurement is taken at 5 μs in the afterglow of the laser-produced helium plasma, and the spectrometer looks directly toward the plasma center. The peak intensity of the distant forbidden line shown in (b) is ~1/20 that of the allowed line shown in (a).

self-absorption observed for the 5876 Å line causes no serious difficulties. We do not use this line for density determination but only to obtain values of the electron temperature from the integrated line intensity, as discussed previously. In this case even a substantial error in intensity causes but a minor error in the temperature.

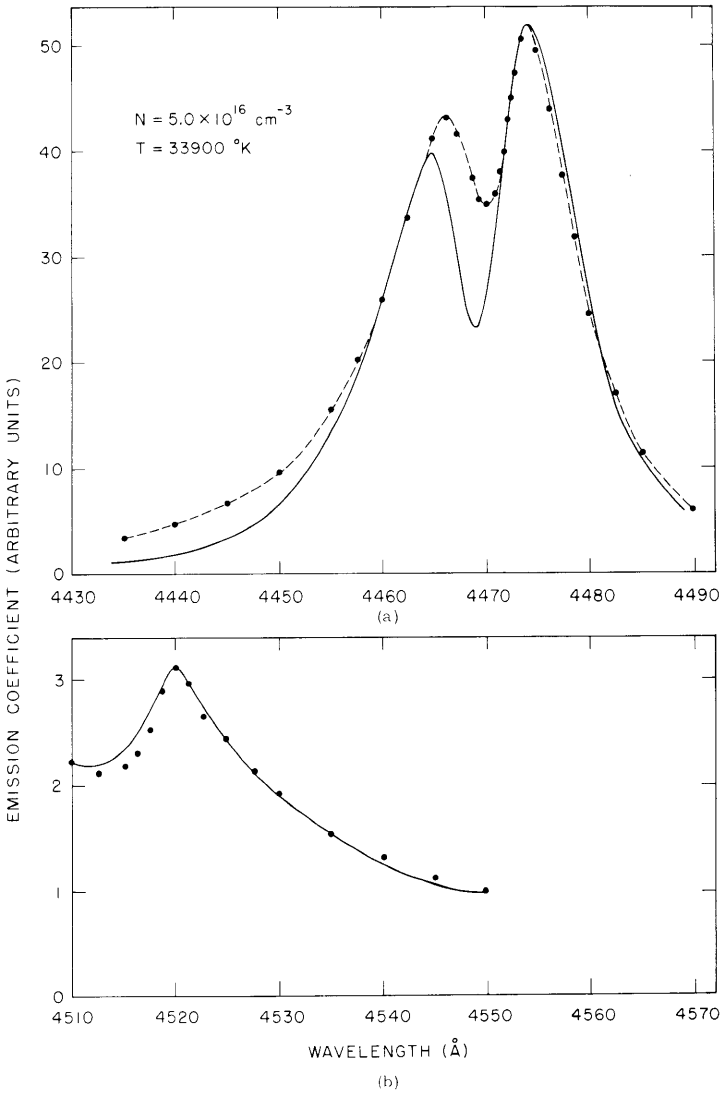

Fig. VI-7. Profiles of the allowed 2^3P-4^3D and the forbidden 2^3P-4^3F transitions (a), and the forbidden 2^3P-4^3P transition (b). The results refer to a radial position within the plasma, r = 0.10 cm. The points denote Abel-inverted experimental data and the dashed line merely connects the pertinent experimental values. The solid line is from theory[1] and has been calculated for values of N and T determined independently (see text).

Figure VI-6 illustrates a typical recorder output of the three helium lines of central concern to this report. At the top of the figure we have the 2^3P-4^3D allowed line almost completely merged with the 2^3P-4^3F forbidden component. At the bottom of the figure we have the distant forbidden line, 2^3P-4^3P. The plots refer to the case when the spectrometer looks directly toward the plasma center. Good signal-to-noise ratio is evident even for the distant forbidden line whose peak intensity is only about 5% that of the allowed line.

We have obtained data like that shown in Fig. VI-6 for some 20 lateral positions of the plasma cigar, and by Abel inversion derived the "true" profiles at various radial positions r. In this report we selected two positions, where the plasma densities N and electron temperatures T have the following values (as determined by

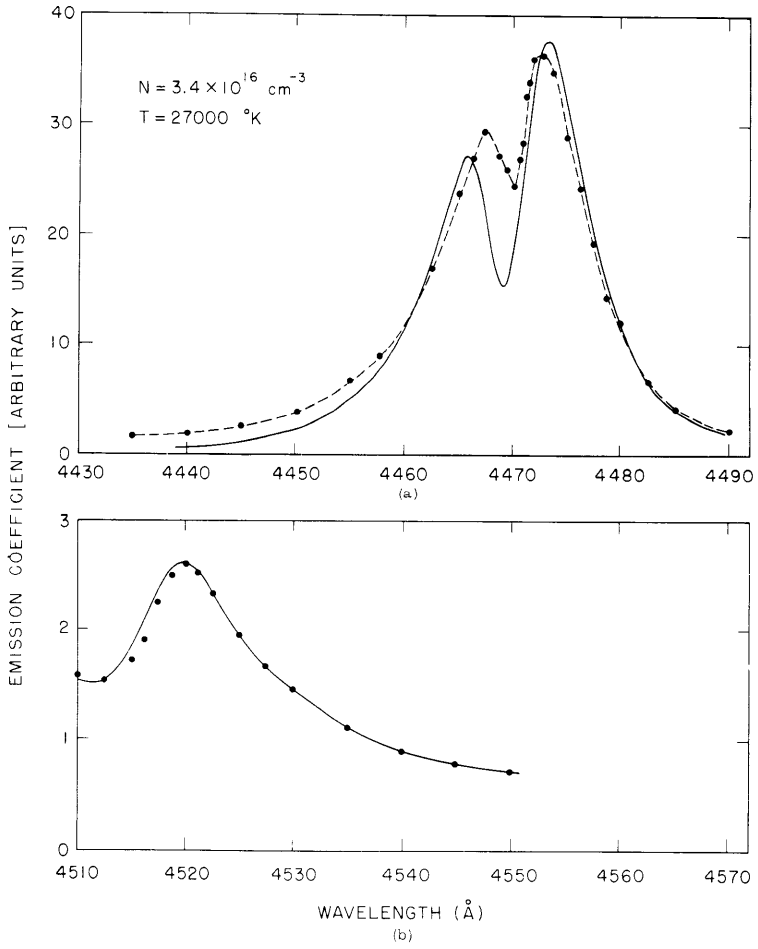

Fig. VI-8. Profiles of the allowed 2^3P-4^3D and the forbidden 2^3P-4^3F transitions (a), and the forbidden 2^3P-4^3P transition (b). The results refer to a radial position within the plasma, r = 0.16 cm.

the aforementioned methods):

$$r_1 = 0.10 \text{ cm}; \quad N = 5.0 \times 10^{16} \text{ cm}^{-3}; \quad T = 33,900°\text{K}$$

$$r_2 = 0.16 \text{ cm}; \quad N = 3.8 \times 10^{16} \text{ cm}^{-3}; \quad T = 27,000°\text{K}.$$

Comparisons between experiment and theory are shown in Figs. VI-7 and VI-8 for the two radial positions in question. The solid points represent the Abel-inverted measurements. The solid lines represent theoretical profiles of the $2^3P\text{-}4^3D, {}^3F, {}^3P$ lines computed by the same methods employed earlier by Griem.[1] In these computations we use the values of temperature and density stated above (with the exception of the value $N = 3.8 \times 10^{16}$ cm^{-3} at r_2 which we replace by $N = 3.4 \times 10^{16}$ cm^{-3}; this gives somewhat better agreement with theory, but the new choice of density lies well within the 15% error brackets quoted earlier).

Discussion

Figures VI-7 and VI-8 show that all is well with regard to the distant forbidden $2^3P\text{-}4^3P$ line, but that something is certainly amiss with regard to the $2^3P\text{-}4^3D, {}^3F$ pair of lines. Here we find discrepancies between experiment and theory very similar to those observed by Nelson and Barnard.[9] Whereas the overall halfwidth of the pair of lines agrees well with theory, the detailed structure does not; the observed peak separation is smaller and the dip between the two lines shallower than predicted by theory. It is clear that merely changing the plasma density in the theoretical profile does not lead to better agreement. For example, lowering the density brings the peaks closer together. On the other hand, this makes the total halfwidth too small and the ratio of peak intensities even larger. The wavelength scale of the experimentally determined profile may have a uniform shift of no more than ± 1.0 Å but a shift of this magnitude would leave the discrepancy essentially the same. It may also be thought that the intensity ratio of the peaks is modified by self-absorption and that the filling in of the dip between the peaks is caused by an outer plasma region of relatively low density. We can refute self-absorption as a cause of error since our measurements show convincingly that this is negligible at the time of measurement. Also, line shape errors caused by density gradients should not be a problem since the Abel transformation of our results effectively corrects for the presence of gradients.

We note that the computations in the table of Barnard et al.[2] yield a somewhat smaller peak separation than do our calculations based on the work of Griem.[1] Even here, however, the agreement between theory and experiment is not very satisfactory.

We are thus led to the following conclusions in regard to plasma diagnostics by means of the $2^3P\text{-}4^3D, {}^3F$ pair of lines. To determine the plasma density, it is the halfwidth

which is the most trustworthy. More specifically, at low densities it is the halfwidth of the allowed line alone, and at high densities ($N \gtrsim 1 \times 10^{16}$ cm^{-3}) it is the combined halfwidth of the strongly overlapping allowed and forbidden lines. The wavelength separation between the two peaks is a much less reliable way of obtaining the density. The use of the intensity ratio of the allowed to the forbidden lines as a means of deducing N is good at low densities only ($N < 1 \times 10^{16}$ cm^{-3}). Here the ratio is determined by the ionic fields which mix the 4^3D and 4^3F states, and the ratio is thus a sensitive function of the ambient plasma density. At higher densities, both lines become weaker with increasing N, and their ratio changes but slowly: now electron broadening becomes an important factor in determining the intensity ratio. In this regime of N the use of the intensity ratio is not too reliable, partly because it is relatively insensitive to the magnitude of N, and partly because it is subject to theoretical uncertainties in calculations of the electron contribution to the line broadening.

In contrast to the above, the 2^3P-4^3P forbidden line at 4517 Å is in satisfactory agreement with theory and its exploitation as a diagnostic tool should be examined further.

G. Bekefi, E. V. George, B. Ya'akobi

[Dr. Ya'akobi is a member of the Department of Physics and Astronomy, University of Maryland.]

References

1. H. R. Griem, Astrophys. J. 154, 1111 (1968); M. A. Gieske and H. R. Griem, Astrophys. J. 157, 963 (1969).
2. A. J. Barnard, J. Cooper, and L. J. Shamey, Astron. Astrophys. 1, 28 (1969).
3. A. J. Barnard and J. Cooper, J. Quant. Spectr. Rad. Transfer 10, 695 (1970).
4. D. D. Burgess and C. J. Cairns, J. Phys. B (Atomic and Molecular Phys.) 3, L67 (1970).
5. D. D. Burgess, J. Phys. B (Atomic and Molecular Phys.) 3, L70 (1970).
6. H. R. Griem, J. Phys. B (Comments on Atomic and Molecular Physics) (in press).
7. B. Ya'akobi, E. V. George, G. Bekefi, and R. J. Hawryluk, Quarterly Progress Report No. 102, Research Laboratory of Electronics, M.I.T., July 15, 1971, p. 67.
8. J. W. Birkeland, M. E. Bacon, and W. G. Braun, Phys. Rev. A 3, 354 (1971). A detailed comparison of experiment with theory cannot be made from this paper because the authors did not supply sufficient data on their plasma density and temperature.
9. R. H. Nelson and A. J. Barnard, J. Quant. Spectr. Rad. Transfer 11, 161 (1971).
10. E. V. George, G. Bekefi, and B. Ya'akobi, "Structure of the Plasma Fireball Produced by a CO_2 Laser" (to be published in Phys. Fluids).

VI. PLASMAS AND CONTROLLED NUCLEAR FUSION*

F. High-Temperature Toroidal Plasmas

Academic and Research Staff

Prof. B. Coppi
Dr. D. B. Montgomery†
Prof. G. Bekefi
Prof. A. Bers
Prof. R. A. Blanken
Prof. R. J. Briggs
Prof. L. M. Lidsky
Prof. R. R. Parker
Prof. K. I. Thomassen
Dr. R. Gajewski
Dr. E. Minardi
Dr. L. Ornstein
Dr. P. A. Politzer
Dr. J. Rem
Dr. D. Schram
Dr. D. J. Sigmar
A. Hugenholtz

Graduate Students

E. L. Bernstein
R. Dagazian
D. P. Hutchinson
Y. Y. Lau
M. A. Lecomte
A. R. Millner
M. Simonutti
E. N. Spithas
B. V. Waddell
D. C. Watson

1. FEASIBILITY OF STATIONARY TOKAMAK‡

At present, considerable hope for controlled thermonuclear fusion relies on the Tokamak approach. To generate electric power, continuous operation is desirable, and the feasibility of a steady-state Tokamak would therefore provide a major incentive for further development. The recent discovery of the "bootstrap effect"[1,2] indicates a way to achieve the steady state, since with this effect the toroidal current necessary for equilibrium is driven by the radial pressure gradient of the confined plasma itself rather than by the usual transformer pulse, provided the gradient and a "seed current" are maintained externally. This can be accomplished by neutral particle injection which provides simultaneous mass, current, and heat inputs. Using the build-up theory of ion density and current on injection parallel to the magnetic field,[3] and extending the theory of Bickerton et al.[1] to cover the relevant cases, conditions for the steady-state operation are delineated. The Kruskal-Shafranov stability criterion limits the injection current so that parallel injection alone cannot balance the banana-diffusion losses. For a steady state, additional particle injection without further increase of the current is required; for example, by injection perpendicular to the field, or by pellets.

In this report we wish merely to outline the problem, which will be treated more extensively in a later publication.

The basic relation for the gradient-driven current in the banana regime is

---

*This work was supported by the U.S. Atomic Energy Commission (Contract AT(30-1)-3980).

†Dr. D. Bruce Montgomery is at the Francis Bitter National Magnet Laboratory.

‡This work was supported in part by the U.S. A.E.C. at the Oak Ridge National Laboratory.

$$j_b = -\sqrt{\frac{r}{R}}\,\frac{T}{B_\theta}\,\frac{\partial n}{\partial r}, \tag{1}$$

where the symbols have the usual meanings. A possible derivation of this result has been given in an earlier report.[4] B_θ is the poloidal magnetic field, and through Ampere's law is connected with j_b. It can be shown that a seed current $I_{seed}(r)$ must be provided near r = 0, along with a particle source S, balancing diffusion losses in the steady state:

$$S(r) = -2\pi r D\,\frac{\partial n}{\partial r} \tag{2}$$

with

$$D = \sqrt{\frac{r}{R}}\,B_\theta^{-2}\eta T n(r),$$

where η is the Spitzer resistivity.

These equations and Ampere's law lead to coupled nonlinear equations for n(r) and I(r), the steady-state density and current profiles. The boundary conditions should be $n(0) = n^o$, $I(0) = 0$. In order to obtain an analytical solution, however, one must restrict the calculation to the region

$$r_o \leq r \leq r_p,$$

where r_o is the "source radius," and r_p the plasma radius, prescribe

$$I(r_o) \equiv I_o, \qquad n(r_o) \equiv n_o,$$

and assume that the seed current and particle source are essentially contained in $r \leq r_o$; that is, $I_{seed} = 0$ and S = const. for $r \geq r_o$. Unfortunately, this model does not reveal the extent to which the seed current dominates the behavior of n and I at r = 0.[5]

If the "bootstrap effect" is weak

$$I_o \approx I_{seed}(r_o)$$
$$n_o \approx n(0). \tag{3}$$

Parametrizing I_o and S through

$$\delta \equiv \sqrt{\frac{R}{r_o}}\,\frac{I_o^2}{r_o^2 \pi n_o Tc^2}$$

and

$$\alpha \equiv \frac{8S}{5n_o \eta c^2} \tag{4}$$

(where we have converted to CGS units, and c is the speed of light). Bickerton et al.[1] have solved for $I(r_p)/I_o$ and r_p/r_o as functions of α and δ.

Sufficient conditions for the validity of Eq. 3 are $\alpha \ll 1$, $\alpha\delta \ll 1$. If the "bootstrap effect" is strong, Eq. 3 breaks down and one cannot easily identify the total current at r_o with the seed current and n_o with n(0).

The relative strength of particle-to-current source is measured by the parameter

$$\lambda^2 = \alpha\delta - (1-\alpha)^2 \tag{5}$$

and all results of Bickerton and his co-workers[1] are for $\lambda^2 \gtrsim 0$. With the Kruskal limit on the seed current, however, the injected steady-state Tokamak plasmas are in the regime $\lambda^2 < 0$, $\alpha > 1$, $\delta \leq \delta_{crit} < 1$. The limit $\lambda^2 = 0$ can be reached both from small and large values of the source strength α, for a given seed current δ. The zeros are at

$$\alpha_{1,2} - 1 = \frac{\delta}{2}\left(1 \pm \sqrt{1+4/\delta}\right). \tag{6}$$

It can be shown that for $\alpha < \alpha_1$, $\delta \leq \delta_{crit}$ no physical steady-state solution exists, but for $\alpha \gg 1$, $\delta \leq \delta_{crit} < 1$ a solution does exist, leading to

$$\frac{I(r_p)}{I_o} = \left[\left(1+\frac{2}{\delta}\right)\left(1+\frac{c_1}{\alpha}+0(\alpha^{-2})\right)\right]^{1/2}, \quad \frac{r_p}{r_o} = \left[1+\frac{c_2}{\alpha}+0(\alpha^{-2})\right]^{2/5}, \ \ldots \tag{7}$$

where $c_1 = \frac{\Delta}{2}\ln\frac{\Delta}{\delta} - 1 - \frac{1}{\Delta}$, $c_2 = c_1 + \frac{1}{\Delta}$, and $\Delta = 2 + \delta$. This solution shows the current magnification and the plasma pinching resulting from the seed current and particle input, in this limit. [These results may be somewhat in error quantitatively, since this limit violates the conditions of Eq. 3. Numerical integration, starting at r = 0 rather than at r_o will give precise answers.]

It remains to determine the possible values of α and δ on injection. More physically, Eq. 4 can be written

$$\alpha = \frac{1}{5}\beta_\theta\left(\frac{r_o}{\rho_{\theta i}}\right)^2\frac{\dot{n}_s}{n_o\nu_{ie}}, \tag{8a}$$

$$\delta = \frac{1}{\beta}\frac{I_o^2}{I_T^2}\left(\frac{R}{r_o}\right)^{5/2}, \tag{8b}$$

where β_θ and β are the poloidal and total β, $\rho_{\theta i}$ is the poloidal plasma ion gyro radius, $\dot{n}_s$ is the injected number density per second, ν_{ie} is the ion-electron collision frequency, and I_T is the current generating the toroidal field. If the Kruskal limit is

to be observed at r_o, that is, if $q(r_o) \geq 1$,

$$\delta \leq \delta_{crit} = \frac{1}{\beta}\left(\frac{r_o}{R}\right)^{3/2}.$$

At $\beta_\theta \sim 1$, $\beta \sim (r_p/R)^{3/2}$ and one gets

$$0 < \delta \leq \left(\frac{r_o}{r_p}\right)^{3/2} < 1 \tag{9}$$

for the range of permitted values of δ. ($\delta = 0$ would correspond to zero seed current.) Thus α_2 is determined from Eq. 6 and Eq. 9 as

$$\alpha_2 \approx 1 + \left(\frac{r_o}{r_p}\right)^{3/4} \gtrsim 1$$

and the regime $\lambda^2 < 0$, $\alpha > \alpha_2$ will indeed be of practical interest.

Callen and Clarke[3] have determined $\dot{n}_s$ and $I_o \approx I_{seed}$ as

$$\dot{n}_s = \frac{I_b}{e\lambda_o 4\pi^2 r_p R} H(r)$$

$$I_s = \frac{I_b v_o \tau_s}{\lambda_o \pi} \sqrt{\frac{r_o}{2R_o}} \frac{1}{10}, \tag{10}$$

where $H(r)$ is a form factor depending on toroidal effects, I_b is the injected beam current, $\lambda_o = (n_o \sigma_{\text{charge exchange}})^{-1}$ and τ_s is the slowing down time for a beam ion. Since the slowing down is mainly a result of ion-electron collisions, $\tau_s \approx \nu_{ie}^{-1}$. Note that the effective seed current is much larger than the beam current resulting from a "storage effect." (An injected ion "lives" many times its transit time around the machine before it is thermalized.) From Eq. 10 we find

$$S(r_o) = \int_0^{r_o} 2\pi r \, dr \, \dot{n}_s(r) = \frac{I_b}{e\lambda_o \pi} \sqrt{\frac{r_o}{2R}} \frac{1}{10}$$

and a coupling between the seed current and particle source strength

$$I_s/S = e v_o \tau_s$$

becomes apparent, peculiar to parallel injection. In terms of α and δ this relation is

$$\alpha^2\delta^{-1} \approx 4\,\frac{T_e}{E_b}\,\frac{m}{M}\,\frac{n_o r_o^2 e^2}{mc^2(\nu_{ie}\tau_s)^2}\,\sqrt{\frac{r_o}{R}} \equiv k, \tag{11}$$

where E_b is the beam energy.

It follows that for usual Tokamak densities ($\lesssim 10^{14}/cm^3$) k is a small number. Taking δ to the Kruskal limit in Eq. 9, Eq. 11 becomes

$$\alpha = \sqrt{k\delta_{crit}} \ll 1.$$

Together with Eq. 9 this determines α and δ on parallel injection, leading to $\lambda^2 < 0$ (Eq. 5) and $\alpha < \alpha_1$ (Eq. 6). As mentioned, no physical steady-state solution exists in this regime because such small values of α do not provide a quantity of source particles equaling the banana-diffusion losses given by the flux

$$\langle nv_r \rangle \approx \sqrt{\frac{r_p}{R}}\,\rho_{\theta i}^2 \nu_{ei}\,\frac{n_o}{r_p}, \tag{12}$$

where $\nu_{ei} = (M/m)\nu_{ie}$. A balance can be reached if additional particles are introduced such that

$$\frac{\dot{n}_s}{n_o \nu_{ie}} = 2\sqrt{\frac{r_p}{R}}\,\frac{\rho_{\theta i}^2}{r_o^2}\,\frac{M}{m}$$

or

$$\alpha = \frac{2}{5}\sqrt{\frac{r_p}{R}}\,\frac{M}{m}\,\beta_\theta. \tag{13}$$

With δ restricted by (9) such large values of α lead to well-behaved solutions for n(r) and I(r) characterized by $\lambda^2 < 0$, $\alpha > \alpha_2$, with a large current magnification and plasma pinching given by Eq. 7.

In contrast to these encouraging results is the fact that in practice, although present technology is able to provide sufficient amounts of seed current, the amount of particle input to offset diffusion losses is rather large. For example, to reach

$$\frac{\dot{n}_s}{n_o \nu_{ie}} = 1$$

in a plasma volume of 10^5 cm^3, typically (e.g., for the Ormak-experiment) $\geq 10^{20}$ pps or ≥ 16 A are required.

I wish to thank J. D. Callen for numerous suggestions and discussions, and

am obliged to him and to J. F. Clarke for making their results available prior to publication.

D. J. Sigmar

References

1. R. J. Bickerton, J. W. Connor, and J. B. Taylor, Nature 229, 110 (1971).
2. B. B. Kadomtsev and V. D. Shafranov, Fourth Conference on Plasma Physics and Controlled Nuclear Fusion Research, University of Wisconsin, Madison, Wisconsin, June 17-23, 1971, Paper IAEA CN-28/F10.
3. J. D. Callen and J. F. Clarke, Private communication, 1971.
4. D. J. Sigmar, Quarterly Progress Report No. 101, Research Laboratory of Electronics, M.I.T., April 15, 1971, pp. 88-99.
5. I wish to thank H. Grad for directing my attention to the existence-problem of the steady-state solution at the origin.